We are IntechOpen, the world's leading publisher of Open Access books Built by scientists, for scientists

4,800
Open access books available

122,000
International authors and editors

135M
Downloads

Our authors are among the

154
Countries delivered to

TOP 1%
most cited scientists

12.2%
Contributors from top 500 universities

CLARIVATE ANALYTICS BOOK CITATION INDEX INDEXED

WEB OF SCIENCE™

Selection of our books indexed in the Book Citation Index in Web of Science™ Core Collection (BKCI)

Interested in publishing with us?
Contact book.department@intechopen.com

Numbers displayed above are based on latest data collected.
For more information visit www.intechopen.com

18

Optimization of Digital Breast Tomosynthesis (DBT) for Breast Cancer Diagnosis

Nachiko Uchiyama[1], Takayuki Kinoshita[2], Takashi Hojo[2], Sota Asaga[2], Junko Suzuki[2], Yoko Kawawa[3] and Kyoichi Otsuka[4]
[1]*Research Center for Cancer Prevention and Screening, National Cancer Center, Tokyo*
[2]*Department of Breast Surgery, National Cancer Center, Tokyo,*
[3]*Department of Radiology, National Cancer Center, Tokyo,*
[4]*Siemens Japan K.K., Tokyo,*
Japan

1. Introduction

Recent papers have reported the usefulness of DBT as the latest diagnostic modality for breast cancer [1]-[6]. In this chapter, the author describes clinical evaluation of the usefulness regarding DBT with reference to other diagnostic modalities such as Full Field Digital Mammography (FFDM), contrast-enhanced (CE) MRI, contrast-enhanced (CE) CT, and ultrasound (US) in accordance with preliminary experiences in breast cancer diagnosis.

2. Diagnostic impact of adjunction of Digital Breast Tomosynthesis (DBT) to Full Field Digital Mammography (FFDM) and in comparison with Full Field Digital Mammography (FFDM)

Purpose: To evaluate the diagnostic impact of adjunction of DBT to FFDM and in comparison with FFDM only, in accordance with pathological findings and breast density.

Materials and Methods: This study was approved by the IRB at our institute. 303 women, having 333 lesions, (age 29-84, mean age 54.0 years old) that were recruited for this study gave informed consent. The images were taken as diagnostic mammograms from October in 2009 to October in 2011. 45 cases were referred from other institutions by US and 258 cases were referred by MMG or palpation. Clinical image data were acquired by an a-Se FFDM system with a spatial resolution of 85μm (MAMMOMAT Inspiration, Siemens, Germany).Two-view DBT was performed with the same rotation angle (±25°) and compression pressure as the FFDM. With one-view DBT, the radiation dose was 1.5 times compared to one-view FFDM. The radiation dose, utilizing ACR 156 phantom by FFDM, was 1.20mGy. Images were reconstructed by the shift and add method and the filtered back projection (FBP) method. FFDM and reconstructed slice images of DBT were reviewed at a dedicated workstation (MAMMO Report, Siemens, Germany). Two radiologists and four breast surgeons evaluated the findings by FFDM only and the adjunction of DBT to FFDM before surgery in accordance with BIRADS categories; BIRADS1-2 (no findings or benign),

BIRADS 3 (probably benign, but short-term follow-up or additional diagnostic procedure necessary), and BIRADS 4-5(highly suspicious or definitely malignant and a biopsy necessary). All cases were operated on and confirmed as malignant or borderline lesions pathologically.

Results: 181 cases were diagnosed as fatty or scattered (BIRADS density 1-2) and 122 cases were diagnosed as inhomogeneous dense or dense (BIRADS density 3-4). Of the pathological findings, 186 lesions were diagnosed as Invasive Ductal Carcinoma(IDC), 60 lesions were diagnosed as Ductal Carcinoma in Situ(DCIS), 33 lesions were IDC predominantly Ductal Carcinoma in Situ(DCIS),16 lesions were diagnosed as Invasive Lobular Carcinoma(ILC), 7 lesions were diagnosed as Lobular Carcinoma in Situ (LCIS), 5 lesions each were diagnosed as Mucinous Carcinoma (Muc Ca) and Intraductal Papilloma (IDP), 4 lesions were diagnosed as Apocrine Carcinoma, 3 lesions each were diagnosed as Mixed IDC+ILC and Intracystic Papillary Tumor(ICPT), two lesions each were diagnosed as Invasive Micropapillary Carcinoma(IMPC), DCIS with LCIS, and Phyllodes Tumor, and one lesion each was diagnosed as SCC, ILC with DCIS, ILC predominantly DCIS, ILC predominantly LCIS, and Muc Ca predominantly DCIS (Table1.). With FFDM only, the detection rate was 88.9% (176/198) for breasts with BIRADS density 1-2 and 83.7% (113/135) for breasts with BIRADS density 3-4. The findings by FFDM only were mass (n=142; 42.6%), Focal Asymmetry(FA) (n=31; 9.3%), distortion (n=15; 4.5%), microcalcifications (n=40; 12.0%), microcalcifications with FA (n=8; 2.4%), microcalcifications with distortion (n=7; 2.1%), microcalcifications with mass (n=46; 13.8%), and none (n=44; 13.2%).

With adjunction of DBT to FFDM, the detection rate (BIRADS 3-5) was 97.4% (193/198) for breasts with BIRADS density 1-2 and 94.8% (128/135) for breasts with BIRADS density 3-4. The average detection rate was 86.8% by FFDM only and 96.4% by adjunction of DBT to FFDM. There was a statistically significant difference between the FFDM only and adjunction of DBT to FFDM among BIRADS density 1-2 and BIRADS density 3-4 ($P<0.05$). On the other hand, there was no statistically significant difference according to breast density (FFDM only: P=0.221, 3-4; adjunction of DBT to FFDM: P=0.202).By BIRADS category with FFDM only, 44 lesions (13.2%) were diagnosed as BIRADS 1 or 2, 75 lesions (22.5%) were diagnosed as BIRADS 3, 214 lesions (64.3%) were diagnosed as BIRADS 4 or 5; on the other hand, 12 lesions (3.6%) were diagnosed as BIRADS 1 or 2, 21 lesions (6.3%) were diagnosed as BIRADS 3, 300 lesions (90.1%) were diagnosed as BIRADS 4 or 5 (Table 2.,Fig1).

In addition, regarding radiological findings, diagnostic accuracy was improved in 96 lesions (BIRADS 1-2 to BIRADS 3-5 or BIRADS 3 to BIRADS 4-5). These included 93 mass-related lesions (mass, FA, or distortion) and 3 microcalcifications-related lesions (microcalcifications, microcalcifications and FA, or microcalcifications and distortion). However, diagnostic confidence was improved in cases of microcalcifications-related lesions owing to the presence of masses or focal dense areas with microcalcifications. In addition, by adjunction of DBT to FFDM, 32 more lesions were detected in comparison with FFDM only (Table 3.)

Discussion. According to recent reports, DBT is a useful diagnostic procedure compared to 2D mammography because breast structures are superimposed onto a two-dimensional (2D) image [6]. The outline of the lesion can be potentially obscured. Our preliminary results also indicated that adjunction of DBT to FFDM contributed not only to detecting the lesion, but

also to clarifying the diagnostic accuracy, especially with regard to mass-related lesions. On the other hand, regarding microcalcifications-related lesions, only using DBT slice image, it is difficult to recognize the overview of the clustered microcalcifications and analyze the morphology of each microcalcification's outline at current settings for image acquisition and reconstruction. As a result, adjunction of DBT to FFDM is the best current option. 32 more lesions were detected by adjunction of DBT to FFDM. Not only 14 invasive cancers (IDC n=11, ILC n=2, ILC pred LCIS n=1), but also 18 non-invasive cancerous or borderline lesions (DCIS n=15, LCIS n=1, IDP n=2).

Adjunction of DBT to FFDM was useful to detect early stage breast cancer and it is not affected by breast density.

Conclusion. In this study, the results indicated that adjunction of DBT to FFDM was superior to FFDM only, regarding diagnostic performance.

333 Lesions	**303 cases with**
IDC	n=186
DCIS	n=60
IDC Pred DCIS	n=33
ILC	n=16
LCIS	n=7
Muc Ca	n=5
IDP	n=5
Apocrine Ca	n=4
IDC with ILC	n=3
ICPT	n=3
IMPC	n=2
DCIS with LCIS	n=2
Phyllodes Tumor	n=2
SCC	n=1
ILC with DCIS	n=1
ILC Pred DCIS	n=1
ILC Pred LCIS	n=1
Muc Ca Pred DCIS	n=1
Total	**n=333**

Table 1. Subtypes of Pathological Findings of the Lesions.

FFDM only	**Adjunction of DBT to FFDM**	
BIRADS 1 or 2 n=44	BIRADS 1 or 2	n=12
	BIRADS 3	n=10
	BIRADS 4 or 5	n=22
BIRADS 3 n=75	BIRADS 3	n=11
	BIRADS 4 or 5	n=64
BIRADS 4 or 5 n=214	BIRADS 4 or 5	n=214
Total	**n=333**	

Table 2. Categorical Changes of FFDM Only Vs. Adjunction of DBT to FFDM.

FFDM Only	**Adjunction of DBT to FFDM**	
DCIS	n=22	n=7
IDC	n=13	n=2
LCIS	n=3	n=2
ILC	n=2	n=0
IDP	n=2	n=0
ILC Pred LCIS	n=1	n=0
ICPC	n=1	n=1
Total	**n=44**	**n=12**

Table 3. Missed Lesions in Pathological Findings by FFDM Only Vs. Adjunction of DBT to FFDM.

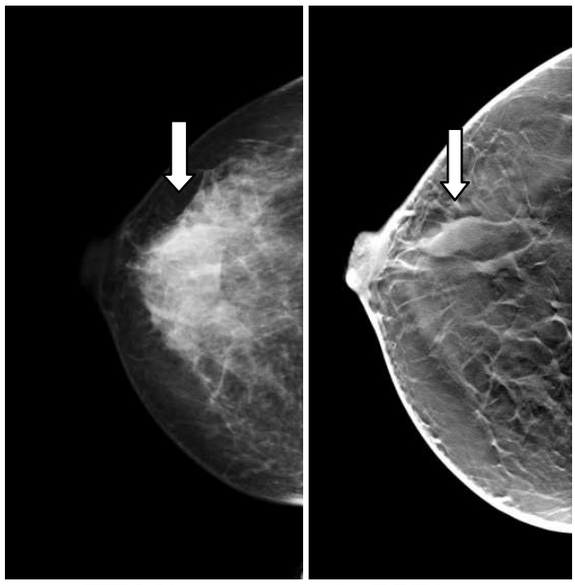

a. FFDM image b. DBT image

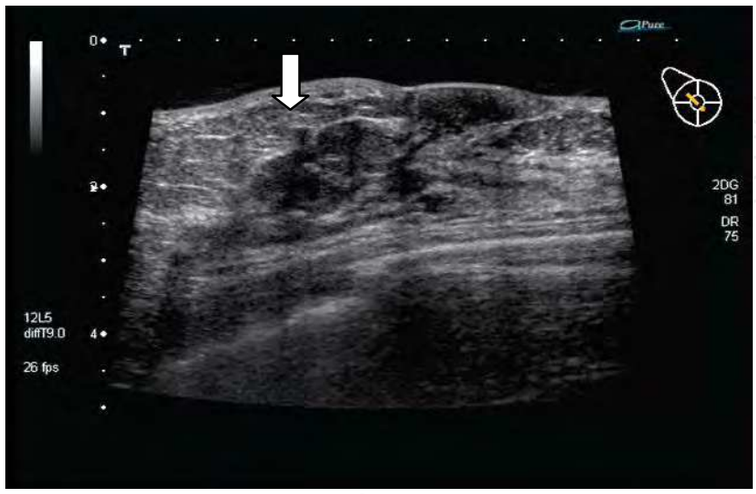

c. US image

Fig. 1. Radiological Findings of Adjunction of DBT and US images.

FFDM (Fig.1a) showed distortion only in the right breast by CC view (white arrow).DBT (Fig.1b) showed an irregularly shaped mass corresponding to the distortion shown by FFDM (white arrow). US (Fig.1c) showed hypo-echoic masses corresponding to the lesion shown by DBT (white arrow). The pathological diagnosis was IDC (Sci Ca).

3. Evaluation of correlation between pathological size and diagnostic size

Purpose

To compare the diagnostic performance between combined Full Field Digital Mammography (FFDM) and Digital Breast Tomosynthesis (DBT) in comparison with US and contrast enhanced MRI with regard to the extent of the lesion.

Materials and methods

This study was approved by the IRB at our institute. 196 women having 217 lesions (age 29-77, mean age 53.0 years old) that were recruited for this study, gave informed consent. The images of FFDM, DBT, US, and contrast enhanced MRI were taken for diagnosis before surgery from October, 2009 to October, 2011. Regarding FFDM and DBT, clinical image data were acquired by an a-Se FFDM system with a spatial resolution of 85μm (MAMMOMAT Inspiration, Siemens, Germany). Two-view DBT was performed with the same compression angle and compression pressure as the FFDM. With one-view DBT, the radiation dose was 1.5 times that of one-view FFDM. The radiation dose, utilizing ACR 156 phantom by FFDM, was 1.20mGy. FFDM and reconstructed slice images of DBT were reviewed at a dedicated workstation. Regarding contrast enhanced MRI, MIP images and MPR images (coronal, axial, sagittal) of 3mm thickness reconstructed from dynamic MRI (four phases) at 3.0 tesla were evaluated. Two radiologists and three breast surgeons evaluated the findings regarding extent of the lesion by FFDM only, FFDM plus DBT, US, and contrast enhanced MRI in a non-blind consensus study before surgery, and compared the total size of the lesion with the actual pathological size of the lesion. The coefficient of correlation was analyzed by Pearson's Product Moment Correlation Coefficient (SPSS Statistics 17.0, IBM, USA).

Results

Of the pathological findings, 125 lesions (57.6%) were diagnosed as IDC, 39 lesions (18.0%) were diagnosed as DCIS, 21 lesions (9.7%) were diagnosed as IDC predominantly DCIS, 11 lesions (5.1%) were diagnosed as ILC, five lesions (2.3%) were diagnosed as LCIS, three lesions each (2.4%) were diagnosed as Muc ca and Apocrine Ca, two lesions each (0.9%) were diagnosed as Phyllodes Tumor and IMPC, one lesion (0.5%) each was diagnosed as ILC with DCIS, Mixed ILC and IDC, Muc Ca pred DCIS, and ICPC(Table1.).The sensitivity of the lesion was 0.908 (197/217) by MMG, 0.972(211/217) by adjunction of DBT to FFDM, 0.927(201/217) by US, and 0.977 (212/217) by MRI.MMG missed 20 lesions (DCIS n=14, IDC n=5, and ICPC n=1), adjunction of DBT to FFDM missed 6 lesions (DCIS n=5 and ICPC n=1), US missed 16 lesions (DCIS n=12, IDC n=2, IDC pred DCIS n=1, and LCIS n=1) , and MRI missed 5 lesions (DCIS n=5).

The coefficient of correlation between pathological diagnostic size and each modality was 0.352 with FFDM ($P<0.01$), 0.586 with adjunction of DBT to FFDM ($P<0.01$), 0.472 with US ($P<0.01$), and 0.628 with MRI ($P<0.01$) regarding IDC and ILC (n=136; pathological size; 3-

108mm, average 35.4mm), 0.516 with FFDM (P<0.05), 0.590 with adjunction of DBT to FFDM (p<0.01), 0.375 with US (P>0.05), and 0.688 with MRI(P<0.01) regarding IDC predominantly DCIS (n=21; pathological size; 14-104mm, average 46.9mm), and 0.454 with FFDM (P<0.01), 0.589 with adjunction of DBT to FFDM (P<0.01), 0.130 with US (P>0.05), and 0.558 (P<0.01) with MRI regarding DCIS(n=39; pathological size; 4-100mm, average 32.6mm) (Fig.2).

Discussion

According to recent reports, CE-MRI is sensitive in evaluating the extent of cancerous lesions; on the other hand, it involves the risk of overestimation of the size of the lesion [7]. In this study, we evaluated the sensitivity and the tumor size determined by FFDM only, adjunction of DBT to FFDM, US, and MRI compared with that determined by pathological diagnosis. In this study, regarding the sensitivity of the lesion, MRI showed the highest sensitivity and adjunction of FFDM to DBT showed comparable performance as well. Regarding the tumor size, MRI showed the strongest correlation with that determined by pathological diagnosis in IDC and ILC (r = 0.628) and IDC pred DCIS (r=0.688). The tumor size determined by adjunction of DBT to FFDM showed the second strongest correlation with that determined by pathological diagnosis in IDC and ILC (r = 0.586) and IDC pred DCIS (r=0.590) and the strongest correlation with that determined by pathological diagnosis in DCIS (r=0.589). By MRI, the lesions of DCIS were over-estimated compared with adjunction of DBT to FFDM (Fig.2c). In addition, the coefficient of correlation between adjunction of DBT to FFDM and MRI showed strong correlation compared to other diagnostic modalities, FFDM only and US. According to the results, the adjunction of DBT to FFDM combined with MRI can contribute to more accurate diagnosis with regard to evaluation of the extent of the lesion.

Conclusion

In this study, the results indicated that the adjunction of FFDM to DBT was superior compared with US or FFDM only, with regard to sensitivity and in evaluating the extent of the lesion. In addition, the adjunction of FFDM to DBT showed a strong correlation with MRI.

	196 Cases 217 Lesions (29-77y.o.; Averag Age 53y.o)
IDC	n=125
ILC	n=11
IDC Pred DCIS	n=21
DCIS	n=39
LCIS	n=5
Muc Ca	n=3
Apocrine Ca	n=3
Phyllodes Tumor	n=2
IMPC	n=2
ILC with DCIS	n=1
Mixed ILC and IDC	n=1
Muc Pred DCIS	n=1
ICPC	n=1
Total	**n=217**

Table 4. Subtypes of Pathological Findings of the Lesions.

FFDM	**Pathology**			
Coefficient of Correlation	0.352**			
Significant Probability	P<0.001			
***** FFDMDBT**	**Pathology**	**FFDM**		
Coefficient of Correlation	0.586**	0.632**		
Significant Probability	P<0.001	P<0.001		
US	**Pathology**	**FFDM**	**FFDMDBT**	
Coefficient of Correlation	0.472**	0.480**	0.583**	
Significant Probability	P<0.001	P<0.001	P<0.001	
MRI	**Pathology**	**FFDM**	**FFDMDBT**	**US**
Coefficient of Correlation	0.628**	0.424**	0.586**	0.660**
Significant Probability	P<0.001	P<0.001	P<0.001	P<0.001

***FFDMDBT: Adjunction of DBT to FFDM

a. IDC,ILC (n=136) (Pathological Size; 3-108mm, Average 35.4mm)

FFDM	**Pathology**			
Coefficient of Correlation	0.516*			
Significant Probability	0.017			
FFDMDBT	**Pathology**	**FFDM**		
Coefficient of Correlation	0.590**	0.932**		
Significant Probability	0.005	P<0.001		
US	**Pathology**	**FFDM**	**FFDMDBT**	
Coefficient of Correlation	0.375	0.587**	0.589**	
Significant Probability	0.094	0.005	0.005	
MRI	**Pathology**	**FFDM**	**FFDMDBT**	**US**
Coefficient of Correlation	0.688**	0.869**	0.909**	0.542*
Significant Probability	0.001	P<0.001	P<0.001	0.011

b. IDC Predominantly DCIS (n=21) (Pathological Size; 14-104mm, Average 46.9mm)

FFDM	**Pathology**			
Coefficient of Correlation	0.454**			
Significant Probability	0.004			
FFDMDBT	**Pathology**	**FFDM**		
Coefficient of Correlation	0.589**	0.883**		
Significant Probability	P<0.001	P<0.001		
US	**Pathology**	**FFDM**	**FFDMDBT**	
Coefficient of Correlation	0.130	0.202	0.272	
Significant Probability	0.431	0.217	0.094	
MRI	**Pathology**	**FFDM**	**FFDMDBT**	**US**
Coefficient of Correlation	0.558**	0.535**	0.699**	0.266
Significant Probability	P<0.001	P<0.001	P<0.001	0.101

* Coefficient of correlation is significant at a 5% standard
** Coefficient of correlation is significant at a 1% standard

c. DCIS (n=39) (Pathological Size; 4-100m, Average 32.6mm)

Table 5. Coefficients of Correlation among Pathological Sizes and Diagnostic Sizes.

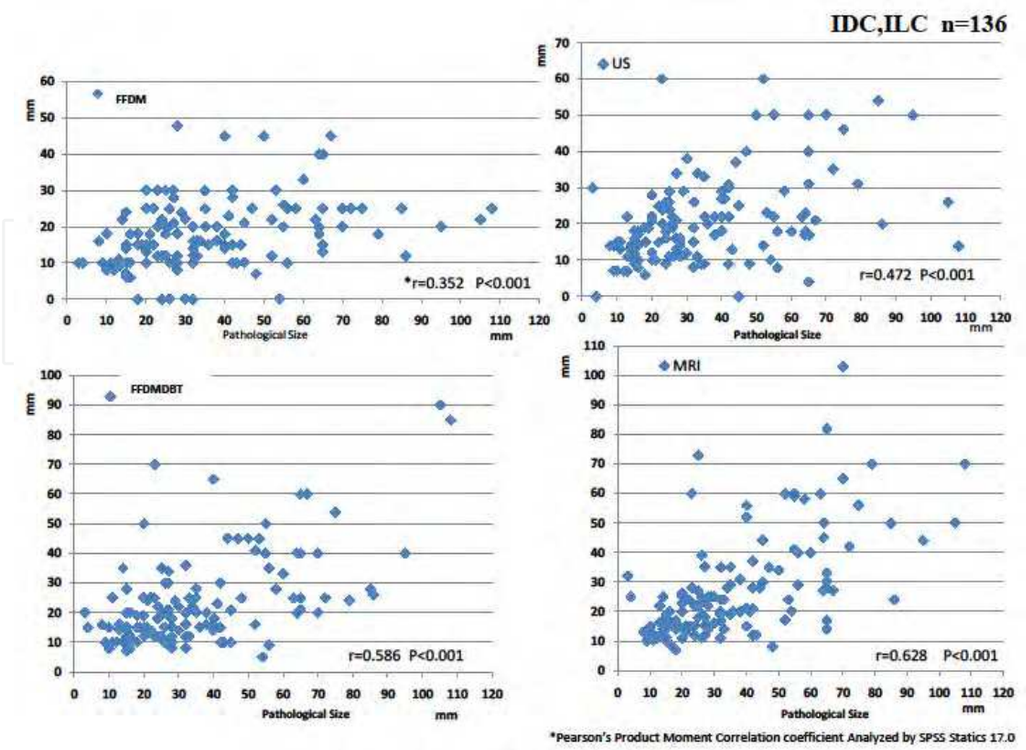

a. Coefficients of Correlation regarding IDC and ILC

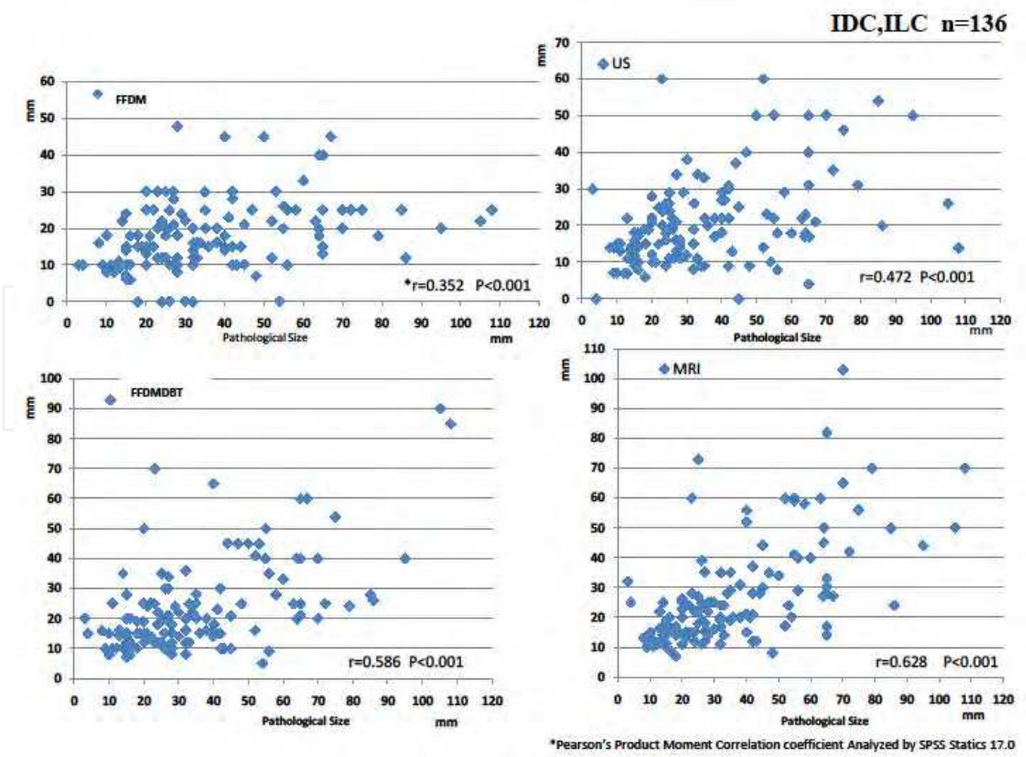

b. Coefficients of Correlation regarding IDC pred DCIS

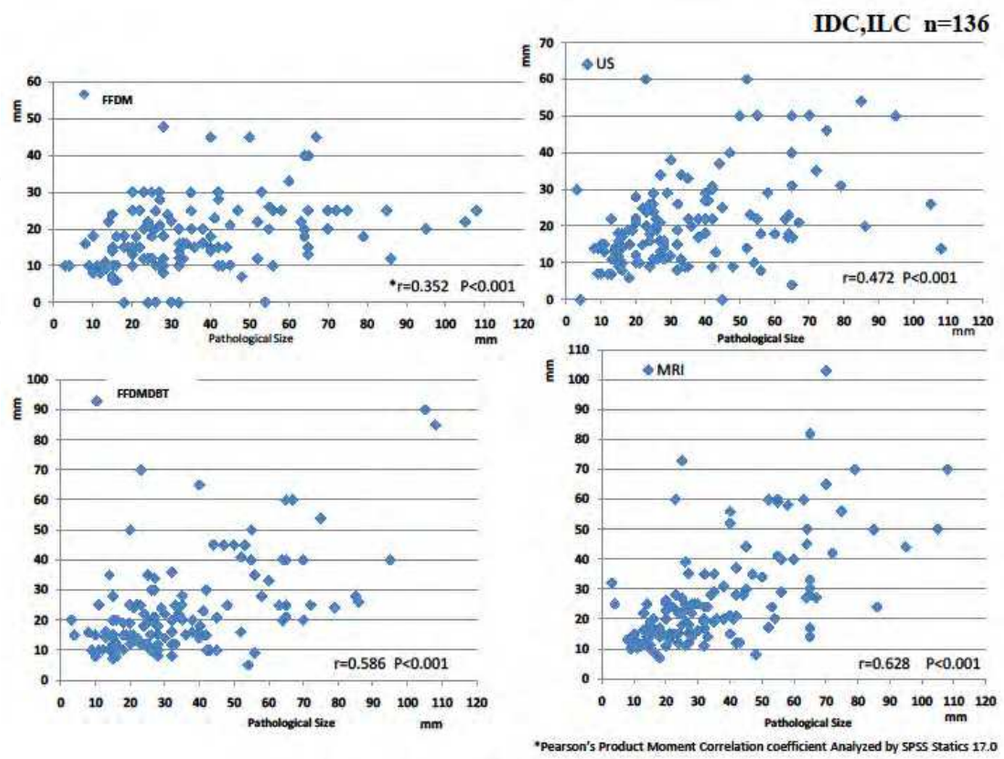

c. Coefficients of Correlation regarding DCIS

Fig. 2. Scatter diagrams of coefficients of correlation among pathological sizes and diagnostic sizes.

4. Usefulness of adjunction of Digital Breast Tomosynthesis (DBT) to Full-Field Digital Mammography (FFDM) in evaluation of pathological response after Neoadjuvant Chemotherapy (NAC) for breast cancer

Purpose

Neoadjuvant chemotherapy (NAC) is performed to reduce tumor size prior to surgery in women with breast cancer. The imaging methods that have been used until now to assess tumor response to neoadjuvant chemotherapy have serious limitations; for example, mammography alone cannot identify mass lesions in very dense breasts or distinguish viable residual lesions from the surrounding fibrous reaction after NAC [8]-[10]. Digital breast tomosynthesis has been only recently applied clinically and the diagnostic advantages in comparison to mammography have been reported on, including the fact that the slice images can be evaluated because tomosynthesis decreases the overlap in breast tissue [1]-[6]. In this study, we assessed the radiological findings and capability of DBT in adjunction to FFDM to predict response to chemotherapy in comparison with other diagnostic modalities.

Materials and methods

This study was approved by the IRB at our institute. 25 women (ages 29-73, mean age, 53.0 years old) having 26 lesions were recruited for this study and gave informed consent. The

images were taken for diagnosis from December, 2009 to October, 2011. Pathological diagnosis was confirmed by Core Needle Biopsy (CNB) and the pathological subtypes were Invasive Ductal Carcinoma (n=20), Invasive Lobular Carcinoma (n=3), Invasive Micropapillary Carcinoma (n=2), and Mucinous Carcinoma (n=1).The clinical stages of the patients before NAC were II or III. All patients underwent surgery based on their response to NAC and residual tumor size estimated by diagnostic imaging was compared with the residual tumor size determined by surgical pathology. The diagnostic procedures were performed within one month prior to surgery. MMG and US were performed on each of the patients before and after NAC. Contrast-enhanced MRI was performed on 15 patients, and contrast-enhanced CT was performed on 10 patients both before NAC and after NAC. Adjunction of DBT to FFDM was performed before and after NAC in 10 out of 25 cases. In 15 out of 25 cases, adjunction of DBT to FFDM was performed only after NAC. Whole-breast US was performed with an 8 MHz wide-band high-resolution transducer (aplio™ XV, Toshiba Medical Systems, Japan). Transverse and longitudinal scans were acquired. Breast MRI was performed with a 3-Tesla system (Magnetom Trio, Siemens, Germany).Patients were studied in the prone position with a dedicated breast surface coil. The entire breast was imaged once before and four times after intravenous injection of 0.1mmol of Gd-DTPA/Kg of body weight (Magnevist; Schering, Germany). The post-processing procedures included digital image subtraction, Maximum Intensity Projection (MIP) and Multiplanar Reconstruction (MPR) by slices of 3mm thickness. Breast CT was performed with multi-detector raw CT (MDCT) (Aquilion64, Toshiba Medical Systems, Japan). The images were acquired before injection an iodine contrast medium, and 60 seconds after, and 3 minutes after injection of the total amount of 100ml, at the rate of 3ml/second (Iopamidol 300, Bayer AG, Germany). The images were reconstructed as slices of 2mm thickness and evaluated. With regard to DBT and FFDM, clinical image data were acquired by an a-Se FFDM system with a spatial resolution of 85μm (MAMMOMAT Inspiration, Siemens, Germany).Two-view DBT was performed with the same compression angle and compression pressure as the FFDM. With one-view DBT, the radiation dose was 1.5 times compared to one-view FFDM. The radiation dose with ACR 156 was 1.2mGy with FFDM. FFDM and reconstructed 1mm slice images from DBT were reviewed at a dedicated workstation. Two radiologists and four breast surgeons evaluated the findings of each diagnostic modality before surgery. The clinical response to chemotherapy was classified into the following categories, based on the "response evaluation criteria in solid tumors" (RECIST), using the measurements obtained with the different imaging methods: 1) Responders: a: Complete Response (CR): no clinical evidence of residual tumor or b: Partial Response, (PR), reduction in size of the tumor by more than 30%; 2) Non-Responders : a: Stable disease (SD): reduction in size of the tumor by less than 30% or b: Progressive disease (PD): increase in size of tumor or presence of new lesions. Pathological response to chemotherapy was classified into four categories: Grade 0 (No Response), Grade 1(Slight Response), Grade 2 (Fair Response), and Grade 3 (Complete Response) [11].

Results

Pathological responses of the lesions to NAC were Grade 0 (n=1), Grade 1 or Grade 2 (n=21), and Grade 3 (n=4).MMG findings of pathological Grade 3 were microcalcifications only (n=1), scar only (n=1), and microcalcifications with reduced mass lesion (n=2). Two out of four (50.0%) lesions demonstrated CR, and two out of four lesions demonstrated PR (50.0%).

Regarding the Grades 1-2 cases, lesions were diagnosed as reduced mass with or without microcalcifications (n=19) demonstrated PR (19/21, 90.5%) and 2 lesions diagnosed as only distortion or scar demonstrated CR (2/21, 9.5%). Regarding the Grade 0 case, the lesion detected as an enlarged mass (n=1) was diagnosed as PD (1/1, 100.0%). Adjunction of DBT findings of pathological Grade 3 were microcalcifications only (n=1), Scar only (n=1), and microcalcifications with scar without any density (n=2) that suggest CR (Fig.1). Regarding pathological Grades 1-2, the lesions were detected as reduced masses with or without microcalcifications (n=20) that suggested 20 cases were PR (20/21, 95.2%), and 1 case of only distortion or scar (n=1) that suggested CR (1/21, 4.8%). Regarding the Grade 0 case, the lesion was detected as an enlarged mass (n=1) that suggested PD (1/1, 100.0%). US findings of pathological Grade 3 (n=4) were diagnosed as CR (n=2, 50.0%), SD (n=1, 25.0%) and PR (n=1, 25.0%). US findings of pathological Grades 1-2 (n=21) were diagnosed as PR (n=17, 81.0%), SD (n=3, 14.3%) and CR (n=1, 4.8%). In the case of US findings of pathological Grade 0 (n=1), the lesion was diagnosed as PD (n=1, 100.0%). MRI (n=15) findings of pathological Grade 3 (3 lesions) were diagnosed as CR (n=2, 66.7%) and PR (n=1, 33.3%). MRI (n=15) findings of pathological Grades 1-2 (11 lesions) were diagnosed as PR (n=10, 90.5%) and CR (n=1, 9.5%). In the case of MRI findings of Grade 0(n=1), the lesion was diagnosed as PD (n=1, 100.0%). CT (10 cases with 11 lesions) findings of pathological Grade 3 (n=1) were diagnosed as CR (n=1, 100.0%). CT findings of pathological Grades 1-2 (n=10) were diagnosed as PR (n=10, 100.0%). MMG only resulted in two under-diagnosed lesions (2/26, 7.7%) and two over-diagnosed lesions (2/26, 7.7%).US resulted in one under-diagnosed lesion (1/26, 3.8%) and five over-diagnosed lesions (5/26, 19.2%). MRI resulted in one under-diagnosed lesion (1/15, 6.7%) and one over-diagnosed lesion (1/15, 6.7%) (Table1).

Discussion

Accurate evaluation of tumor response to NAC is necessary for optimization of preoperative planning. MRI and CT have recently developed the potential to assist the other traditional imaging methods in the evaluation of response to NAC [12]-[20]. By mammography, it is difficult to identify a mass lesion in dense breasts or to distinguish a viable lesion from a fibrous reaction owing to NAC. Using US only can result in over-diagnosis of chemotherapy-induced fibrosis, because in the case of a hypo-echoic lesion, it is difficult to differentiate between a fibrotic change induced by neoplastic change and a reduction in the tumor by NAC. In addition, it is difficult to measure by hand-held probe the overview of a large mass lesion or multi-centric lesions, such as locally advanced tumors that could be treated by NAC (Fig.1). On the other hand, adjunction of DBT to FFDM has potential diagnostic advantages. In accordance with our study, compared to FFDM only, adjunction of DBT to FFDM can evaluate the inside of and the outline of the lesion. Compared to US, adjunction of DBT to FFDM can evaluate the overview of the lesion objectively. Accurate evaluation of tumor response to the pharmacological treatment is fundamental for optimal surgical planning. CE-MRI and CE-CT have recently developed the potential to assist the other traditional imaging methods in the evaluation of response to chemotherapy. These are able to discriminate between neoplastic and fibrotic tissue, based on the rate of contrast media enhancement [12]-[17]. In addition, the higher sensitivity of MRI can detect non-invasive lesions as enhanced lesions that can be over-diagnosed as residual invasive components (Fig.2). According to our study, compared to CE-CT or CE-MRI, with adjunction of DBT to FFDM, it is possible to correlate the macroscopic evaluation with the pathological diagnosis without utilizing a contrast medium. The combination of adjunction

of DBT to FFDM with other diagnostic modalities will contribute to improved diagnostic accuracy with regard to NAC response to locally advanced breast cancer.

Conclusion

The adjunction of DBT to FFDM combined with other diagnostic modalities will contribute to more accurate assessment of pathological response to NAC.

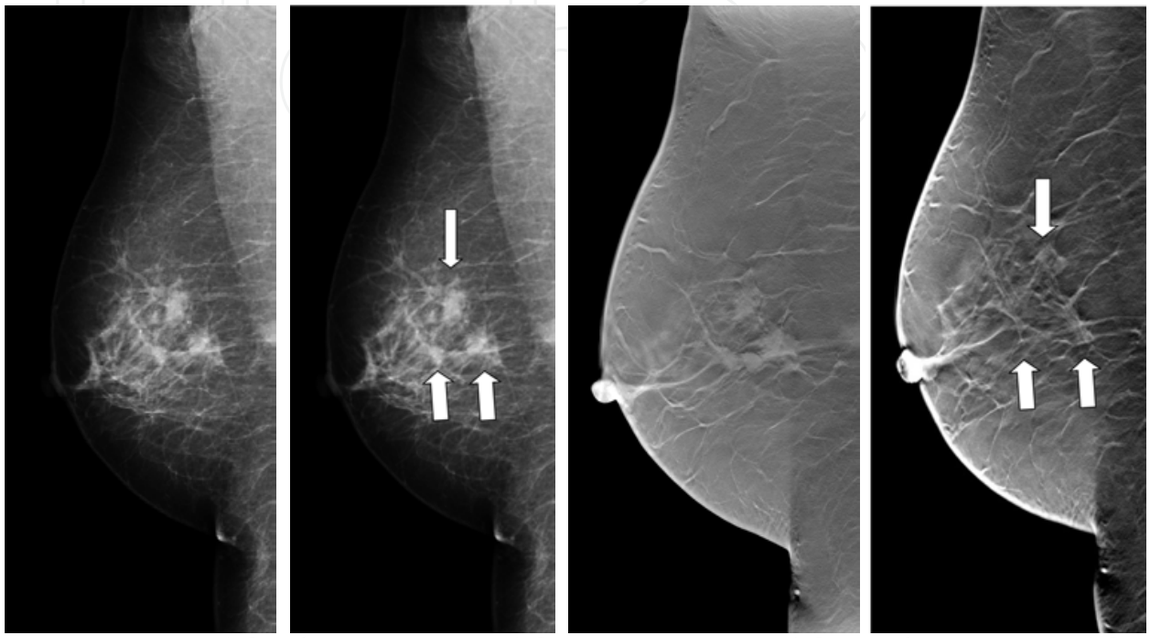

a. FFDM: Pre NAC b. FFDM: Post NAC c. DBT: Pre NAC d. DBT: Post NAC

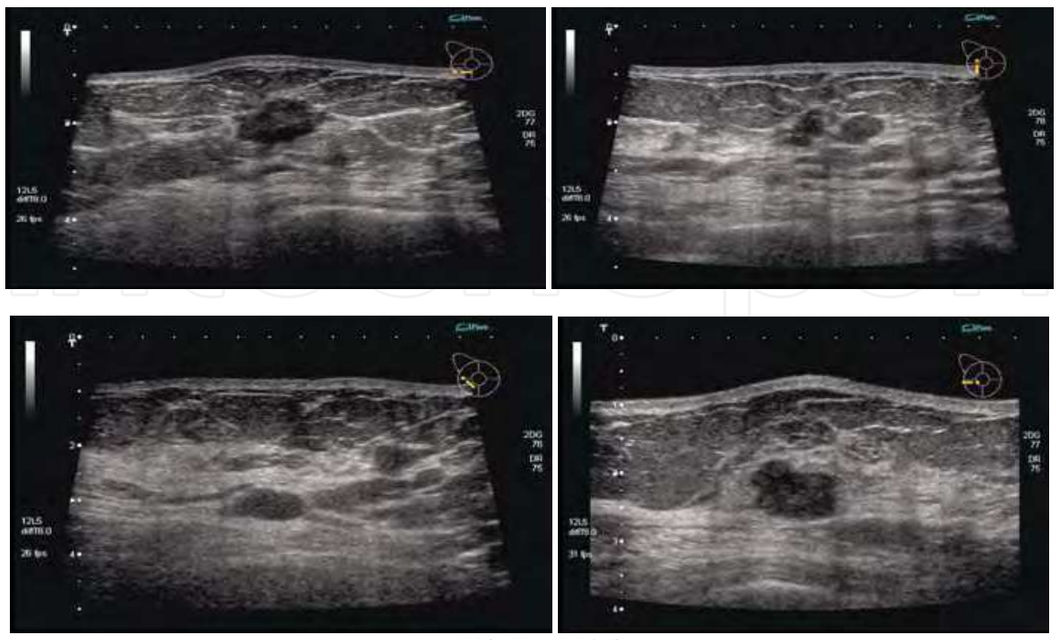

e. US: Pre NAC

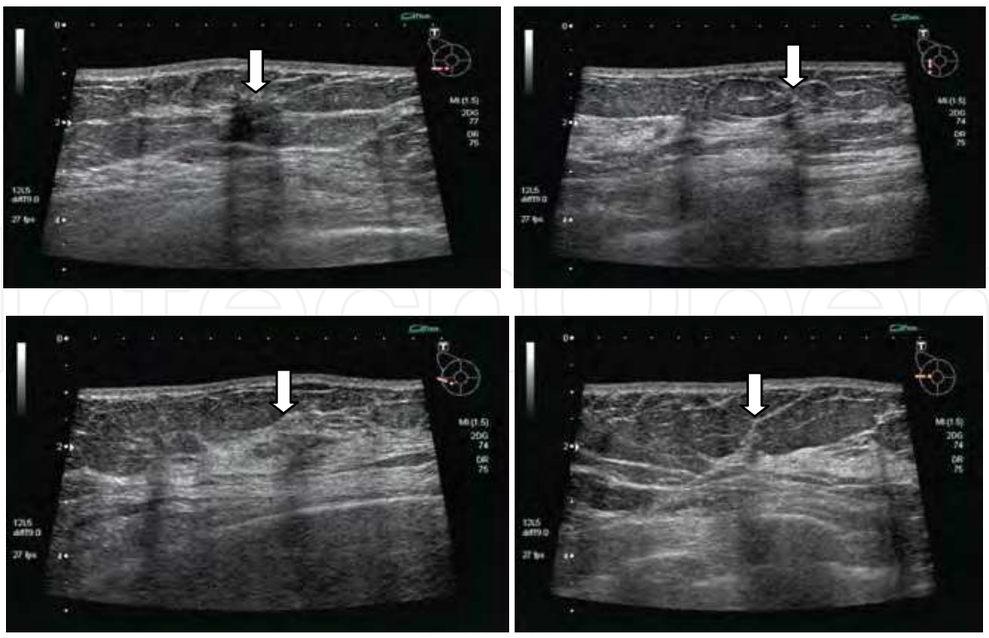

f. US: Post NAC

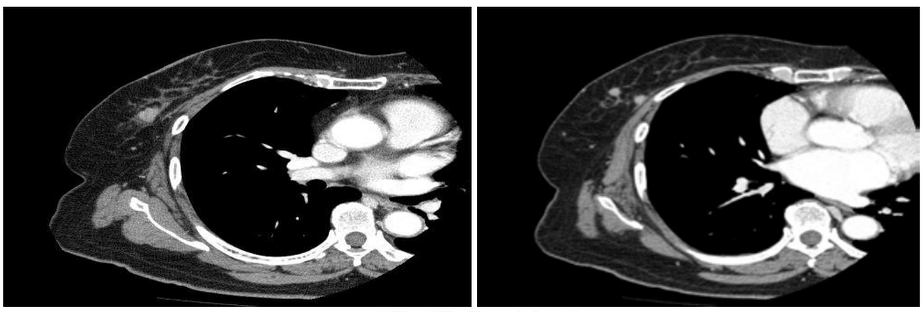

g. CE-CT: Pre NAC

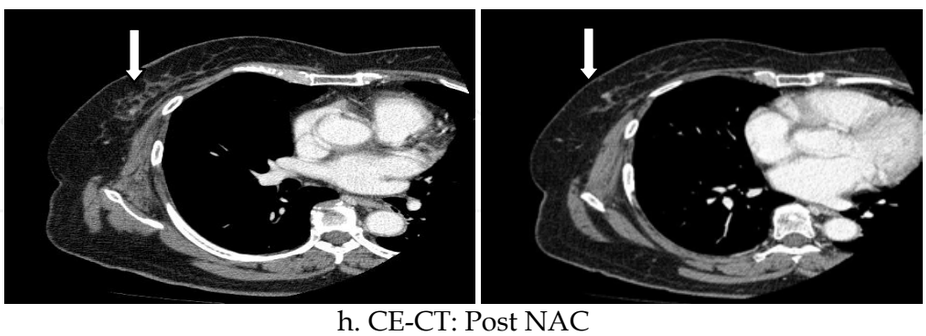

h. CE-CT: Post NAC

FFDM (Fig.1a-b) showed reduced masses after NAC (white arrow).
DBT (Fig.1c-d) showed reduced masses with scar with partial density inside of the corresponding lesion after NAC (white arrow).
US (Fig.1e-f) showed reduced hypo-echoic masses as suspicious residual lesions after NAC (white arrow).
The images of CE-CT (Fig.1g-h) showed reduced small enhanced nodules as suspicious residual lesions after NAC (white arrow).

Fig. 3. Pathological Grade 1 Case.

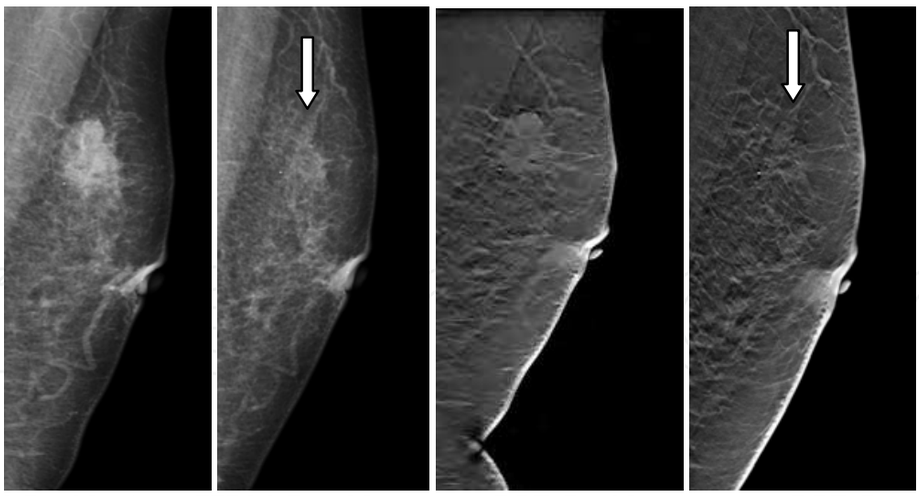

a. FFDM: Pre NAC b. FFDM: Post NAC c. DBT: Pre NAC d. DBT: Post NAC

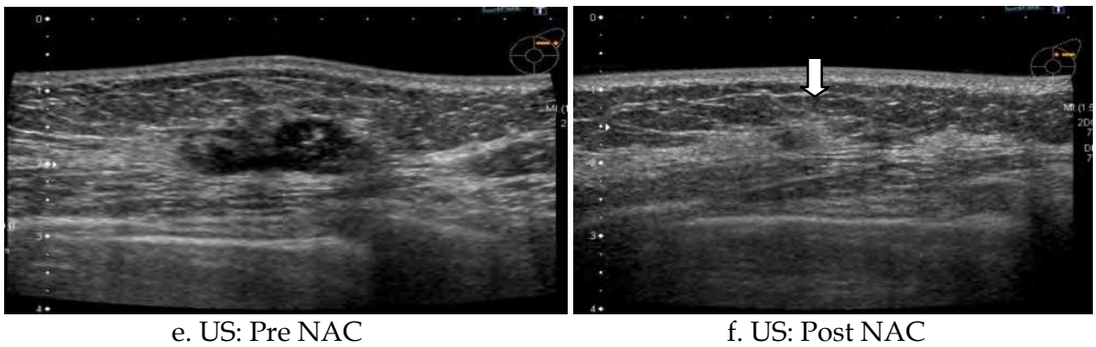

e. US: Pre NAC f. US: Post NAC

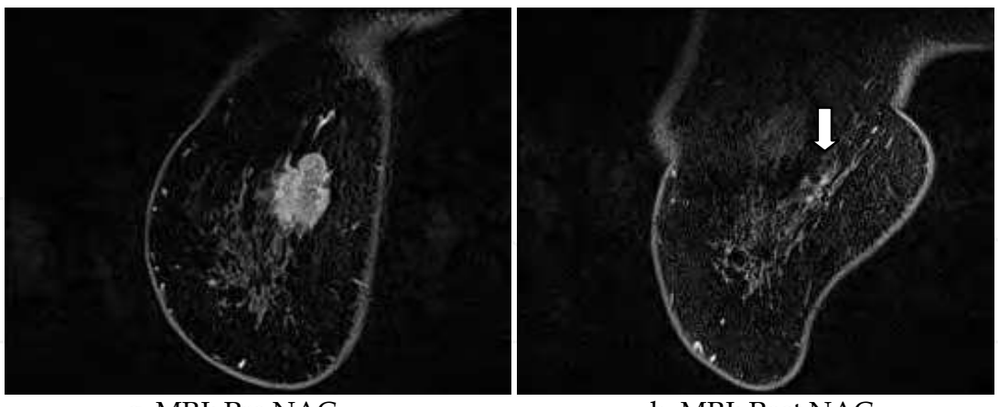

g. MRI: Pre NAC h. MRI: Post NAC

FFDM (Fig.2a-b) demonstrated a reduced mass with microcalcifications after NAC (white arrow).
DBT (Fig.2c-d) demonstrated microcalcifications with scar without core density inside of the corresponding lesion after NAC (white arrow).
US (Fig.2e-f) demonstrated a reduced hypo-echoic mass as a suspicious residual lesion after NAC (white arrow).
The coronal image of CE-MRI (Fig.2g-h) demonstrated small enhanced nodules as a suspicious residual lesion after NAC (white arrow). Pathological diagnosis demonstrated residual DCIS corresponding to the enhanced lesions by CE-MRI.

Fig. 4. Pathological Grade 3 Case.

Pathological Response	**MMG**	**US (n=26)**
Grade 0 (n=1)	*PD: n=1(100.0%)	PD: n=1(100.0%)
Grades 1-2 (n=21)	PR: n=19(90.5%), CR: n=2(9.5%)	PR: n=17(81.0%), SD: n=3(14.3%), CR: n=1(4.8%)
Grade3 (n=4)	CR: n=2(50.0%), PR: n=2(50.0%)	CR: n=2(50.0%), PR: n=1(25.0%), SD: n=1(25.0%)
Pathological Response		**CT (n=11)**
Grades 1-2 (n=10)		PR: n=10 (100.0%)
Grade 3 (n=1)		CR: n=1 (100.0%)
Pathological Response		**MRI (n=15)**
Grade 0 (n=1)		PD: n=1(100.0%)
Grades 1-2 (n=11)		PR: n=10(90.9%), CR: n=1(9.1%)
Grade 3 (n=3)		CR: n=2(66.7%), PR: n=1(33.3%)

* The clinical response to chemotherapy was classified in accordance with RECIST.

Table 6. Comparison of NAC Response by Diagnostic Evaluation and Pathological Evaluation.

5. Acknowledgment

This study was supported by Grant-in-Aid for Scientific Research (C) (No. 23591810) in Japan.

6. References

[1] Poplack SP, Tosteson TD, Kogel CA et al. (2007). Digital breast tomosynthesis: initial experience in 98 women with abnormal digital screening mammography. AJR 189(3): 616-23.

[2] Andersson I, Ikeda DM, Zackrisson S, et al. (2008). Breast tomosynthesis and digital mammography: a comparison of breast cancer visibility and BIRADS classification in a population of cancers with subtle mammographic findings. Eur Radiol 18(12): 2817-25.

[3] Good WF, Abrams GS, Catullo VJ, et al. (2008). Digital breast tomosynthesis: a pilot observer study. AJR 190(4): 865-9.

[4] Gennaro G, Toledano A, di Maggio C, et al. (2010) Digital breast tomosynthesis versus digital mammography: a clinical performance study. Eur Radiol. 20(7):1545-53.

[5] Uchiyama N, Kinoshita T, Akashi S, et al.(2011) Diagnostic Performance of Combined Full Field Digital Mammography (FFDM) and Digital Breast Tomosynthesis (DBT) in comparison with Full Field Digital Mammography (FFDM). CARS2011:32-33, Springer.

[6] Förnvik D, Zackrisson S, Ljungberg O, et al. (2010).Breast tomosynthesis: Accuracy of tumor measurement compared with digital mammography and ultrasonography. Acta Radiol. 51(3):240-7.

[7] Berg WA, Gutierrez L, NessAiver MS, et al.(2004).Diagnostic accuracy of mammography, clinical examination, US, and MR imaging in preoperative assessment of breast cancer. Radiology. 233(3):830-49.

[8] Helvie MA, Joynt LK, Cody RL, et al. (1996) Locally advanced breast carcinoma: accuracy of mammography versus clinical examination in the prediction of residual disease after chemotherapy. Radiology 198:327–332.

[9] Moskovic EC, Mansi JL, King DM, et al. (1993) Mammography in the assessment of response to medical treatment of large primary breast cancer. Clin Radiol 47:339–344.

[10] Keune JD, Jeffe DB, Schootman M, et al.(2010) Accuracy of Ultrasonography and Mammography in Predicting Pathologic Response after Neoadjuvant Chemotherapy for Breast Cancer. Am J Surg. 199(4): 477–484.

[11] Therasse P, Arbuck SG, Eisenhauer EA, et al. (2000) New Guidelines to evaluate the response to treatment in solid tumors. JNCI 92:205–216.

[12] Abraham DC, Jones RC, Jones SE, et al. (1996) Evaluation of neoadjuvant chemotherapeutic response of locally advanced breast cancer by Magnetic Resonance Imaging. Cancer 78:91–100.

[13] Londero V, Bazzocchi M, Del Frate C, et al. (2004)Locally advanced breast cancer: comparison of mammography, sonography and MR imaging in evaluation of residual disease in women receiving neoadjuvant chemotherapy. Eur Radiol. 14:1371–1379.

[14] Rosen EL, Blackwell KL, Baker JA, et al.(2003).Accuracy of MRI in the detection of residual breast cancer after neoadjuvant chemotherapy.AJR. 181:1275–1282.

[15] Yeh E, Slanetz P, Kopans D. (2005) Prospective Comparison of Mammography, Sonography, and MRI in Patients Undergoing Neoadjuvant Chemotherapy for Palpable Breast Cancer. A J R. 184:868–877.

[16] Balu-Maestro C, Chapellier C, Bleuse A, et al. (2002) Imaging in evaluation of response to neoadjuvant breast cancer treatment benefits of MRI. Breast Cancer Res Treat. 72:145–152.

[17] Partridge SC, Gibbs JS, Lu Y, et al.(2002) Accuracy of MR imaging for revealing residual breast cancer in patients who have undergone neoadjuvant chemotherapy. A J R. 179:1193–1199.

[18] Akashi T S, Fukutomi T, Sato N, et al.(2004) The use of contrast-enhanced computed tomography before neoadjuvant chemotherapy to identify patients likely to be treated safely with breast-conserving surgery. Ann Surg. 239(2):238-43.

[19] Vinnicombe SJ, MacVicar AD, Guy RL et al. (1996) Primary breast cancer: mammographic changes after neoadjuvant chemotherapy, with pathologic correlation. Radiology 198:333–340.

[20] Tozaki M, Kobayashi T, Uno S, et al. (2006) Breast-conserving surgery after chemotherapy: value of MDCT for determining tumor distribution and shrinkage pattern. AJR. 186(2):431-9.

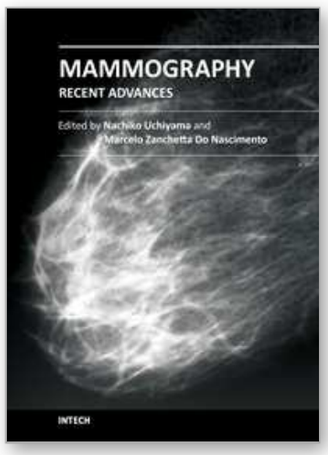

Mammography - Recent Advances
Edited by Dr. Nachiko Uchiyama

ISBN 978-953-51-0285-4
Hard cover, 418 pages
Publisher InTech
Published online 16, March, 2012
Published in print edition March, 2012

In this volume, the topics are constructed from a variety of contents: the bases of mammography systems, optimization of screening mammography with reference to evidence-based research, new technologies of image acquisition and its surrounding systems, and case reports with reference to up-to-date multimodality images of breast cancer. Mammography has been lagged in the transition to digital imaging systems because of the necessity of high resolution for diagnosis. However, in the past ten years, technical improvement has resolved the difficulties and boosted new diagnostic systems. We hope that the reader will learn the essentials of mammography and will be forward-looking for the new technologies. We want to express our sincere gratitude and appreciation?to all the co-authors who have contributed their work to this volume.

INTECH
open science | open minds

InTech Europe
University Campus STeP Ri
Slavka Krautzeka 83/A
51000 Rijeka, Croatia
Phone: +385 (51) 770 447
Fax: +385 (51) 686 166
www.intechopen.com

InTech China
Unit 405, Office Block, Hotel Equatorial Shanghai
No.65, Yan An Road (West), Shanghai, 200040, China
中国上海市延安西路65号上海国际贵都大饭店办公楼405单元
Phone: +86-21-62489820
Fax: +86-21-62489821

IntechOpen